Electronic Supplementary Information

Flexible Large-Area Electrochromic Devices with Enhanced Cycling Stability Enabled by Ni/MnO_2 Hybrid Mesh Electrodes

Mengnan Wang,[a] Chunyang Su,[a] Yinuo Du,[b] Waner Liu,[b] Shiqing Zhao[b] and Yanhua Liu*[a]*

[a.] School of Optoelectronic Science and Engineering, Key Lab of Advanced Optical Manufacturing Technologies of Jiangsu Province & Key Laboratory of Flexible Optoelectronics and Micro/Nano Manufacturing of Jiangsu Province, Soochow University, Suzhou 215006, P. R. China.

[b.] Key Laboratory of Efficient Low-carbon Energy Conversion and Utilization of Jiangsu Provincial Higher Education Institutions, School of Physical Science and Technology, Suzhou University of Science and Technology, Suzhou 215009, P. R. China.

Electronic mails: sqzhao@usts.edu.cn; yhliu@suda.edu.cn

1. Calculation formula of coloration efficiency (CE)

$$CE = \frac{\Delta OD}{\Delta Q} = \frac{\log(\frac{T_b}{T_c})}{\Delta Q} \quad \text{* MERGEFORMAT (S1)}$$

In this equation S1, ΔOD is the change of optical density, ΔQ is the inserting/extracting electronic charge, T_b and T_c are the transmittance of the bleached and colored state, respectively.

2. Calculation formula of Ion diffusion coefficient

$$i_p = kn^{\frac{3}{2}} AD^{\frac{1}{2}} cv^{\frac{1}{2}} \quad \text{* MERGEFORMAT (S2)}$$

In this equation S2, i_p is the current density of the oxidation-reduction peak, A is the electrode area, D is the diffusion coefficient, c is the ion concentration, n is the number of exchange electrons, v is the scan rate, k is the Randles-Sevick constant, equal to 2.69×10^5.

TABLE S1. Ion diffusion rate.

Sample	D_{in} (cm^2/S)	D_{out} (cm^2/S)
PET/ITO/WO_3	1.76×10^{-11}	6.95×10^{-12}
PET/Ni mesh/WO_3	9.00×10^{-11}	3.00×10^{-12}

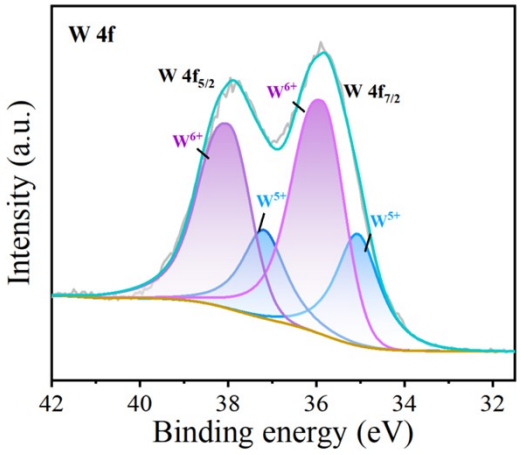

Fig. S1 XPS spectra of WO_3 thin films prepared by magnetron sputtering after coloring: W 4f spectrum.

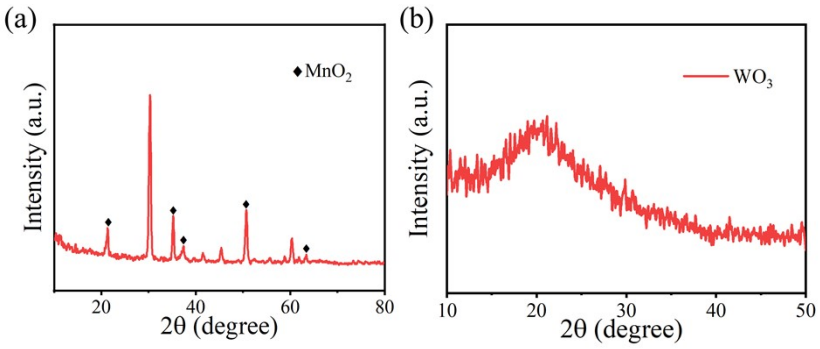

Fig. S2 XRD patterns: (a) MnO_2, (b) WO_3.

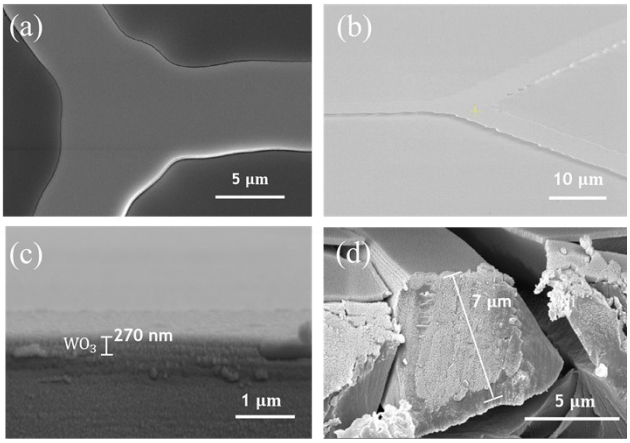

Fig. S3 (a) SEM image of PET/Ni mesh/WO_3 sample surfaces. (b) SEM image with inclination state at 10°, (c) and (d) are cross-section SEM images of the sample.

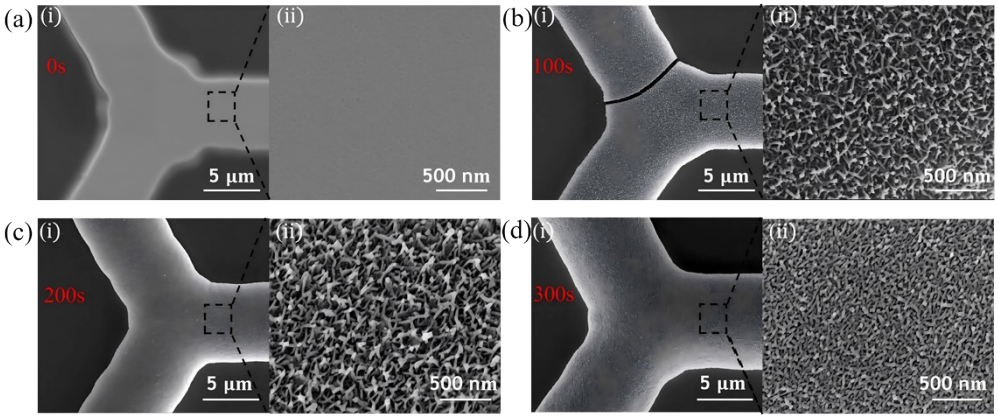

Fig. S4 Characterization diagram of the microstructure of the PET/Ni/MnO_2 mesh electrode. SEM images of mesh electrodes prepared by depositing MnO_2 on Ni mesh electrodes for 0 s (a), 100 s (b), 200 s (c), and 300 s (d), respectively (where Figure (i) shows the appearance of the hybrid mesh electrode and Figure (ii) shows the microstructure of MnO_2).

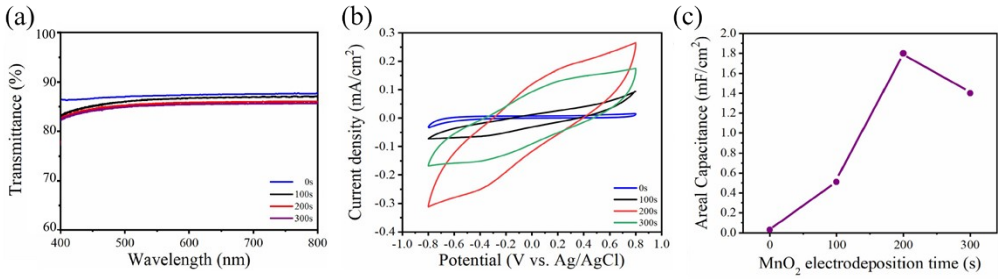

Fig. S5 (a) Transmittance curves and (b) cyclic voltammetry curves of PET/Ni/MnO_2 mesh electrodes with different MnO_2 deposition times. (c) Specific capacitance of PET/Ni/MnO_2 mesh electrodes with different MnO_2 deposition times (Voltage ±0.8 V, sweep rate 50 mV/s).

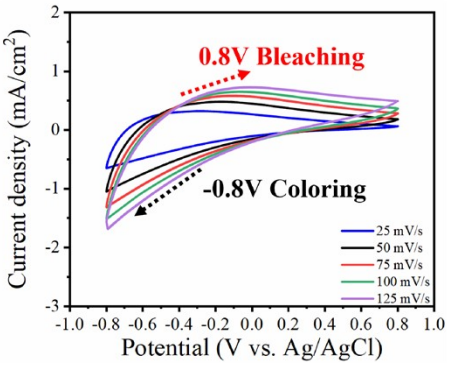

Fig. S6 Cyclic voltammetry curves of PET/ITO/WO_3 sample in 1 mol/L $LiClO_4$/PC with arrows indicating the scanning direction.

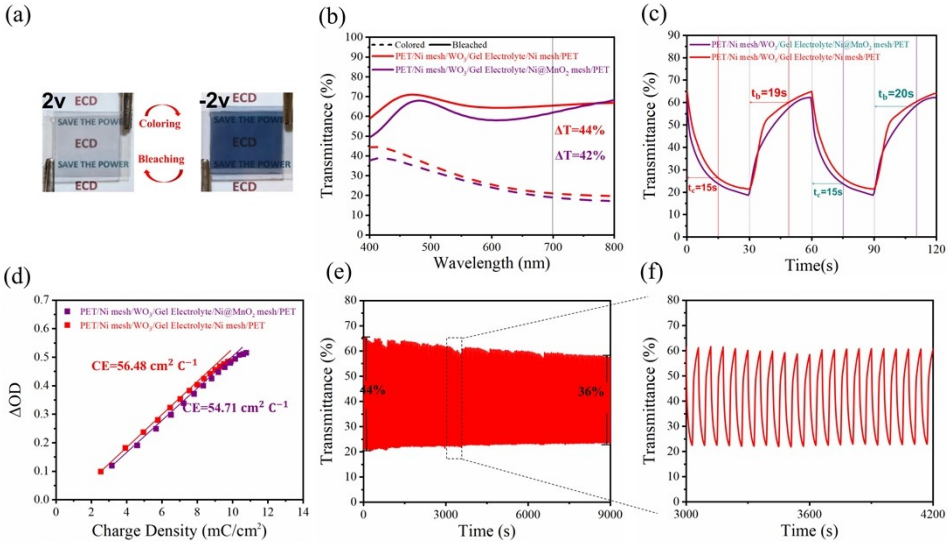

Fig. S7 (a) Images of PET/Ni mesh based flexible electrochromic devices for coloring and bleaching. (b) Transmittance curves and (c) response time curves of PET/Ni mesh and PET/Ni/MnO_2 mesh based flexible electrochromic devices for coloring and bleaching. (d) Density versus charge density curves. (e) Transmittance curves of PET/Ni mesh based flexible electrochromic device at 700 nm with coloring and bleaching cycle. (f) Detail curves of coloring and bleaching cycle variation at 700 nm for PET/Ni mesh based flexible electrochromic devices.

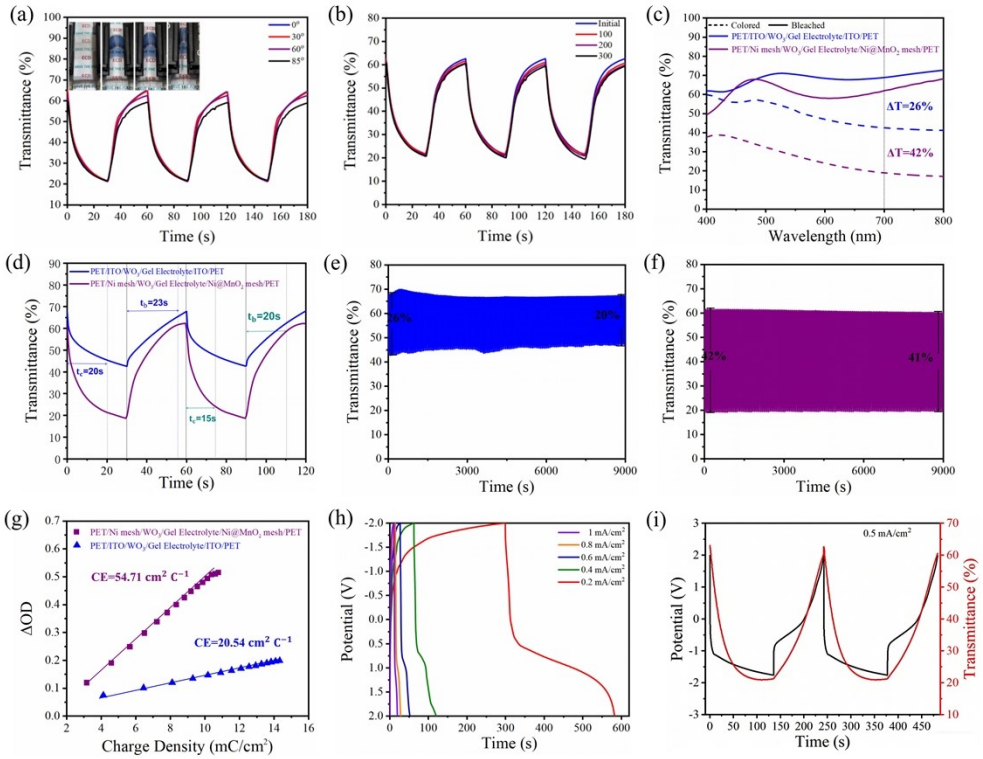

Fig. S8 (a) Transmittance versus coloring and bleaching cycle curves of PET/Ni mesh based flexible electrochromic devices under the bending angles of 0°, 30°, 60°and 85°, respectively (inset is the corresponding images of the four bending states). (b) Transmittance versus coloring and bleaching cycle curves of PET/Ni mesh based flexible electrochromic devices after 100, 200 and 300 times of bending with the bending angle 60°. (c) The transmittance curves and (d) response time curves for PET/ITO and PET/Ni/MnO_2 mesh based devices during coloring and bleaching. (e) The transmittance curves of PET/ITO and (f) PET/Ni/MnO_2 mesh electrode varies with the coloring-bleaching cycle at 700 nm. (g) Optical density as a function of the charge density for PET/ITO and PET/Ni/MnO_2 mesh based devices at 700 nm. (h) GCD curves of PET/Ni/MnO_2 mesh based devices at different current densities from 0.2 to 1 mA/cm^2. (i) GCD versus transmission cycling curve at a current density of 0.2 mA/cm^2.

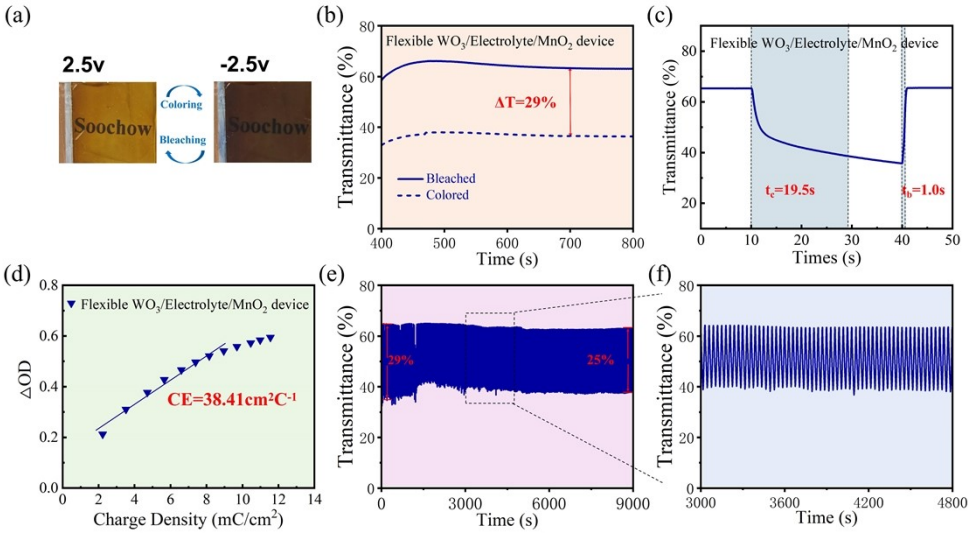

Fig. S9 (a) Images of PET/ITO electrode based flexible electrochromic devices for coloring and bleaching. (b) Transmittance curves and (c) response time curves of PET/ITO/MnO_2 electrode based flexible electrochromic devices for coloring and bleaching. (d) Density versus charge density curves. (e) Transmittance curves of PET/ITO electrode based flexible electrochromic device at 700 nm with coloring and bleaching cycle. (f) Detail curves of coloring and bleaching cycle variation at 700 nm for PET/Ni mesh based flexible electrochromic devices.